NOAA Technical Memorandum ERL WPL-34

DEPARTMENT OF COMMERCE
UNITED STATES OF AMERICA

INFRARED PASSIVE WIND SENSING - A FEASIBILITY STUDY

G. R. Ochs
Ting-i Wang

Wave Propagation Laboratory
Boulder, Colorado
October 1977

noaa NATIONAL OCEANIC AND ATMOSPHERIC ADMINISTRATION / Environmental Research Laboratories

Printed for Atmospheric Sciences Laboratory,
U.S. Army Electronics Command, White Sands Missile Range,
New Mexico 88002, as Research and Development Technical Report
ECOM-77-10. Approved for public release; distribution unlimited.

NOAA Technical Memorandum ERL WPL-34

INFRARED PASSIVE WIND SENSING - A FEASIBILITY STUDY

G. R. Ochs
Ting-i Wang

The primary support for this project was provided by the U.S. Army Electronics Command, Atmospheric Sciences Laboratory, White Sands, N. M. 88002, under contract W43P6S 77-8029. The Scientific Monitor was Mr. Ruben Rodriques.

Wave Propagation Laboratory
Boulder, Colorado
October 1977

UNITED STATES
DEPARTMENT OF COMMERCE
Juanita M. Kreps, Secretary

NATIONAL OCEANIC AND
ATMOSPHERIC ADMINISTRATION
Richard A. Frank, Administrator

Environmental Research
Laboratories
Wilmot N. Hess, Director

CONTENTS

INFRARED PASSIVE WIND SENSING - A FEASIBILITY STUDY

G. R. Ochs and Ting-i Wang

We analyze the feasibility of measuring crosswinds by observing the scintillation of the natural background radiation in the wavelength region from 8 to 12 microns. Methods of signal analysis and experimental results for visual wavelengths are discussed. A signal-to-noise analysis and experimental results indicate that an infrared system is marginally possible, with S/N ratios approximately two orders of magnitude below that of a visual system.

1. INTRODUCTION

A study of the feasibility of measuring crosswinds by observing the scintillation of the natural background radiation has been completed as part of the requirements of a research contract (MIPRW43P6S 77-8029) with the U.S. Army Electronics Command, Atmospheric Sciences Laboratory, White Sands, New Mexico. Dr. Donald L. Walters of ASL originally suggested the possibility of measuring winds in this way. The obvious advantage of such a system, of course, would be its ability to operate at night as well as in the daytime. It appeared that such a system might indeed be workable, as scintillation had been observed in infrared imaging systems. Also the background radiation should be more constant than daytime illumination at visual wavelengths. Passive wind measurement systems operating in the visual or near infrared suffer large changes in signal-to-noise (S/N) because the illumination and the refractive-index structure constant (C_n^2) tend to be correlated near the ground.

These advantages, however, are offset by other considerations. In general, the scintillation is less at the longer wavelengths, though it may not be for certain arrangements using incoherent illumination. More serious is the reduced energy in the radiation at longer wavelengths. The effective S/N of the best infrared detectors in the 8-11 micron region is much less than that of a low-priced photodiode operating in the 0.3-1.1 micron region.

We chose the 8-11 micron region since the background radiation is most intense here; however strong arguments also exist for the 3 and 5 micron windows because of the detectors available in these regions.

2. NEW PASSIVE TECHNIQUES

2.1 Theory

Preliminary calculations indicated that poorer S/N could be expected for the infrared compared to a visible system. Consequently a major portion of the research was devoted to improving passive wind sensing analysis techniques. This work served a dual purpose in that the improved techniques were incorporated in a battery-powered passive wind sensor operating in the 0.8 micron region. The unit, together with an instruction book, was also delivered as part of the research contract.

The analysis technique is based upon a system first described by Ochs and Miller (1972). It has evolved considerably since that time and has been used in active as well as passive units. The technique is particularly useful for analysis of the coherent portion of partially-coherent wideband signals. Additionally, a filter function centered upon the mean frequency of the coherent part of the signals can be specified. The specific application for the passive wind sensor is described by Ochs et al. (1977). Though more complex than the original 1972 system, the present system has the advantages of better S/N and less sensitivity to changes in scene spectrum.

In all of our earlier models, we used the so-called slope technique (Clifford et al., 1975) to measure the crosswind. Essentially, we used only the information of the time-lagged covariance function in the neighborhood of zero delay and disregarded the information contained in the rest of the covariance function. In this report, we use a different method to analyze the measured covariance function. This method, which we shall call the "covariance method", uses the information contained in the whole covariance function to obtain the crosswind.

We sample, at many delays, the time-lagged covariance function of the signals detected by two horizontally separated detectors. The mean frequency of the coherent portion of the signals can be obtained from the cross-covariance function by a lock-on servo circuit. The measured frequency is proportional to the path-averaged absolute value of crosswind. If the wind has opposite directions across various portions of the path, the mean of the absolute wind $|V|$ is not the same as the true mean wind $\overline{V}$. The quantity $|V|$ is defined by

$$\overline{|V|} \equiv \int_{-\infty}^{\infty} |V| \; p(v)dv \; , \qquad (1)$$

where p(v) is the probability density function of the crosswind. To see the difference between $\overline{|V|}$ and $\overline{V}$, we assume that p(v) follows a gaussian probability distribution with mean $\overline{V}$ and standard deviation σ_V, i.e.,

$$p(v) = \frac{1}{\sqrt{2\pi}\,\sigma_V} \, e^{-(v-\overline{v})^2/(2\sigma_V^2)} \; . \qquad (2)$$

Inserting Eq. (2) into Eq. (1), we have

$$\overline{|V|} = \frac{1}{\sqrt{2\pi}\,\sigma_V} \left[\int_{0}^{\infty} dvve^{-(v-\overline{v})^2/(2\sigma_V^2)} - \int_{-\infty}^{0} dvve^{-(v-\overline{v})^2(2\sigma_V^2)} \right]$$

$$= \overline{V} \, \mathrm{erf} \left(\frac{\overline{V}}{\sqrt{2}\,\sigma_V} \right) + \sqrt{\frac{2}{\pi}} \, \sigma_V \, e^{-\overline{v}^2/(2\sigma_V^2)} \qquad (3)$$

where erf( ) is the error function. Equation (3) can be reduced to

$$\overline{|V|} = \alpha \overline{V} \; , \qquad (4)$$

where

$$\alpha = \mathrm{erf}\left(\frac{1}{\sqrt{2}R}\right) + \sqrt{\frac{2}{\pi}} \, R \, e^{-1/(2R^2)} \qquad (5)$$

and $R = \sigma_V/\overline{V}$. The quantity α is the ratio of $\overline{|V|}$ to $\overline{V}$, and α is always greater than unity. From Eq. (5), when R = 1; α = 1.16, this is only a 16% over-estimation of the mean wind even when the standard deviation of the wind along the path is equal to the mean wind. Obviously, this is not a strong restriction on the crosswind measurement.

One of the most troublesome problems encountered in measuring path-averaged crosswinds by an optical scintillometer using a natural scene as a source, is the weak signal-to-noise ratio of the received signals. One way to improve the SNR is to use a detector array as a spatial filter (Clifford et al. 1975). However, in order to prevent saturation problems, an extended incoherent detector-array must be used (Wang et al., 1978) and the large physical size of the detectors may make the optical unit unwieldy.

The new technique, as described in the last section, is not as sensitive to noise as is the slope technique. For the slope technique, we use the normalized covariance function defined by

$$C_{xN}(\tau) = \frac{\langle S_1(t)S_2(t+\tau)\rangle}{\langle S_1^2\rangle^{1/2}\langle S_2^2\rangle^{1/2}} , \qquad (6)$$

where < > denotes the ensemble average, and S_1 and S_2 are the signals from the two detectors. The slope at zero delay (M_N) is obtained by differentiating Eq. (6) with respect to τ and setting $\tau = 0$

$$M_N = \frac{\partial}{\partial\tau}\left[\frac{\langle S_1(t)S_2(t+\tau)\rangle}{\langle S_1^2\rangle}\right]_{\tau=0} . \qquad (7)$$

In Eq. (7), we assume that $\langle S_1^2\rangle = \langle S_2^2\rangle$. From Lawrence et al. (1972) M_N is proportional to the path-averaged wind. Now, let us assume that the detected signals are composed of two components. One is the useful signal $S_i^{'}(i = 1,2)$ and the other is the associated noise N_i. Then Eq. (7) becomes

$$M_N = \frac{\partial}{\partial\tau}\left[\frac{\langle S_1^{'}(t)S_2^{'}(t+\tau)\rangle + \langle N_1(t)N_2(t+\tau)\rangle}{\langle S_1^{'2}\rangle + \langle N_1^2\rangle}\right]_{\tau=0} . \qquad (8)$$

In obtaining Eq. (8) we use the assumptions that the signal $S^{'}$ and the noise are uncorrelated, that $\langle N_1\rangle = \langle N_2\rangle = 0$, and that $\langle N_1^2\rangle = \langle N_2^2\rangle$. Furthermore, if we assume that N_1 and N_2 are uncorrelated (i.e., $\langle N_1N_2\rangle = 0$), then

$$M_N = \frac{\partial}{\partial\tau}\left[\frac{\langle S_1^{'}(t)S_2^{'}(t+\tau)\rangle}{\langle S_1^{'2}\rangle + \langle N_1^2\rangle}\right]_{\tau=0} . \qquad (9)$$

From Eq. (9) it is clear that the measured wind (slope) is a function of SNR when the SNR is small. The larger the noise power, the smaller the slope, so that the measurement underestimates the wind. For a passive system, high noise is unavoidable since we have no control of the target scene. Because in the new technique, we use the covariance function to measure the mean frequency of the correlated portion of the signals, the measured value is insensitive to noise as long as the shape of the covariance curve does not change much. Besides, in the new technique, we sample the covariance at 14 different delays, and the resulting redundancy reduces the effect of random noise.

2.2 Experimental Results

In Figure 1, we compare 1-min averages of the passive crosswind monitor readings with the average of two propeller anemometers reading the wind across the optical path 40 and 80 m from the receiving unit. The crosswind monitor is observing a scene 500 m away. The wind weighting function has been measured over a longer period of time with the same arrangement and the result is shown in Figure 2.

We examined the sensitivity to changes in scene spectrum by turning on a point source of light within the scene. This extreme change in the scene spectrum produced wind readings 25% too high. The older slope analysis was performed simultaneously, and its readings were 100% too high. It should be pointed out, however, that the errors for both systems would be less if the light and the scene were further away.

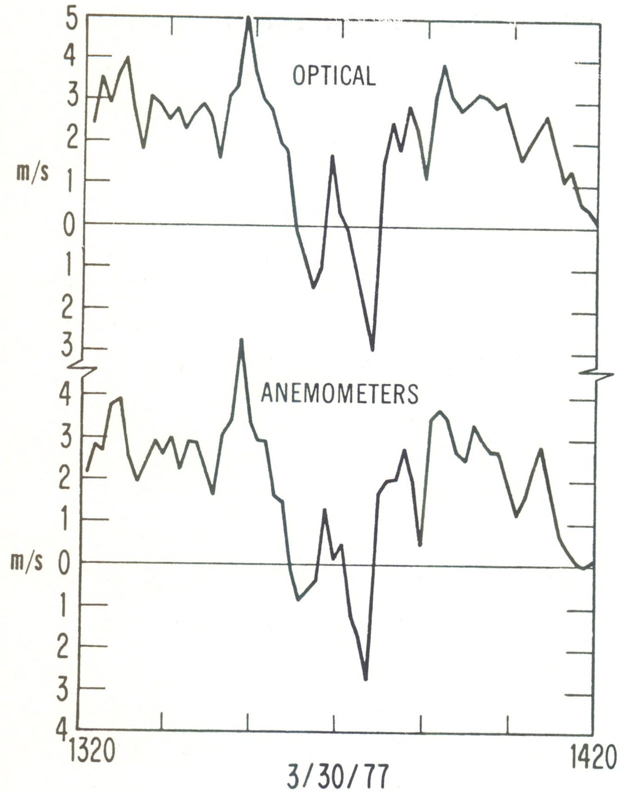

Fig. 1. Comparison of 1-min averages of the passive optical wind reading with the average of two propeller anemometers reading the wind across the optical path 40 and 80 m from the receiver.

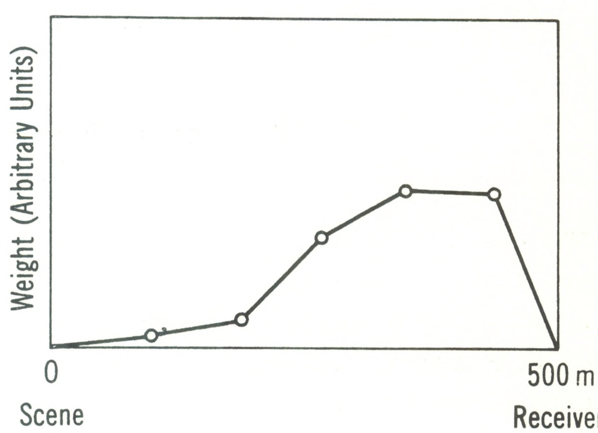

Fig. 2. A typical wind weighting function for the passive optical crosswind monitor.

Although not in the passive mode, long-term comparisons of covariance and slope systems operating with an incoherent light source indicate that the standard deviation of hourly averages of the calibration factor, relative to a 10-anemometer average on a 500-m path, is about 0.06 for the slope method and only 0.02 for the covariance system.

3. PASSIVE WIND SENSING IN THE INFRARED

3.1 Signal-to-noise Analysis

As a first step in predicting the performance of an infrared system, we make a S/N calculation and compare it with that attainable with the visual system. Some unknowns remain, but the uncertainty should be less than an order of magnitude.

We begin by examining the visual system using a PIN SPOT/2D photodiode. The noise equivalent power (NEP) and sensitivity (S) are listed as

$$\text{NEP (5 hz)} < 10^{-12}\ \text{W}$$
$$\text{S (typical)} = 0.4\ \mu\text{A}/\mu\text{W}.$$

In typical operation on a sunny day, the photodiode current (i), for a 15-cm diameter receiving aperture and 3.6 mrad field of view, is approximately 10 μA. So the irradiance (I_V) is

$$I_V = i/S = 2.5 \times 10^{-5}\ \text{W}.$$

If we assume white noise and a 500 Hz bandwidth,

$$\text{NEP (500 Hz)} = 10^{-12}(500/5) = 10^{-10}\ \text{W}.$$

If we estimate a scintillation level = 10^{-4} of the background (typical, although there are enormous variations), we have for the visual system,

$$\text{SNR} = \frac{2.5 \times 10^{-5}}{10^{-10}} \times 10^{-4} = 25.$$

This is somewhat higher than usually observed, but not unreasonable since amplifier noise has not been included.

For the infrared work, we chose a SAT liquid-nitrogen cooled HgCdTe detector, class A2 having an area of 4×10^{-4} cm^2, with half-power response 8 to 11 μm (with filter), and $D^* = 1.65 \times 10^{10}$ cm Hz$^{1/2}$ W^{-1}. The detector was placed at the focus of a Newtonian telescope having a 15 cm diameter aperture and a 27.9 cm focal length, providing a field of view of $4\times10^{-4}/27.9^2 = 5.14 \times 10^{-7}$ ster. The radiance of the scene (Ashley et al., 1975) is taken as 700 μW cm^{-2} ster^{-1} μm^{-1}. The detector irradiance I_{iv} then is

$$I_{iv} = 700\ \mu\text{W cm}^{-2}\text{ster}^{-1}\mu\text{m}^{-1} \times 176.7\ \text{cm}^2 \times 5.14 \times 10^{-7}\text{ster} \times 3\ \mu\text{m} = 1.91 \times 10^{-7}\ \text{W}$$

I_{iv} can also be estimated from the Stefan-Boltzman law

$$I_{iv} = \sigma\theta^4 = 5.672 \times 10^{-12}\ \text{W cm}^{-2}\ \text{deg}^{-4} \times 290^4 \times 176.7\ \text{cm}^2 \times 5.14 \times 10^{-7}$$

$$= 3.64 \times 10^{-6}\ \text{W}$$

which would indicate an emissivity of .05, not unreasonable, especially if some attenuation is also present. We make no wavelength scaling correction because the scintillation in the infrared will not necessarily be lower than that in the visual, for incoherent illumination and receiver apertures larger than the Fresnel zone size (Wang et al., Submitted to JOSA). In fact, the scintillation level will often be lower in the infrared than it is at optical wavelengths because of reduced contrast in the scene. While a contrast ratio of 16:1 (sunlight : open shade) might be expected in the visual, ratios of 2:1 at 10 μm due to temperature differences alone would require a difference of more than 50°C. Nevertheless, differences in emissivity could cause contrast ratios of 2:1. This reasoning leads us to assume a fractional scintillation level of $10^{-4} \times (2/16) = 1.25 \times 10^{-5}$. The noise power expected from the detector will be

$$\text{NEP} = \frac{\sqrt{A\Delta f}}{D^*} = \frac{\sqrt{4 \times 10^{-4}\ \text{cm}^2\ 500\ \text{Hz}}}{1.65 \times 10^{10}\ \text{cm Hz}^{1/2}\text{W}^{-1}} = 2.71 \times 10^{-11}\ \text{W}$$

so the predicted signal-to-noise is, for $I_{iv} = 1.91 \times 10^{-7}$W,

$$S/N = \frac{1.91 \times 10^{-7} \times 1.25 \times 10^{-5}}{2.71 \times 10^{-11}} = 0.09.$$

For $I_{iv} = 3.64 \times 10^{-6}$W, $S/N = 1.7$.

3.2 Experimental Results

The performance estimates in section 3.1 were sufficiently encouraging to warrant the purchase of an infrared detector with the characteristics on which the calculations were based. While an actual wind measurement system would require at least two detectors, one was sufficient to evaluate the prospects. The experimental arrangement is shown in Figure 3. The detector is placed at the focus of an f 1.8 Newtonian telescope. The signal is preamplified at the base of the detector, bandpass filtered to the range 2 - 500 Hz, and then amplified.

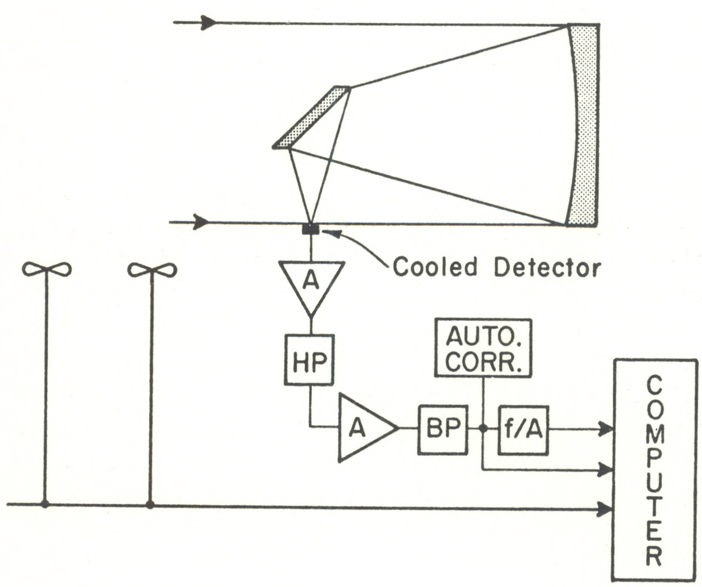

Fig. 3. Test arrangement for experimental evaluation of passive infrared wind sensing.

To align, focus, and check the entire system, a radiation source consisting of a 25-W soldering iron at the focus of a 15-cm concave mirror of 28 cm focal length was pointed at the detector telescope 500 m away. Scintillation was readily observed from this incoherent source, with good S/N. One would expect that the mean frequency of the scintillation would be proportional to the mean of the absolute value of the crosswind. This was indeed the case, and results comparable to those seen at 0.8 μm wavelength were readily obtained. Scintillations were also readily obtained with good S/N from a hot plate and a soldering iron at a range of 80 meters.

Various natural targets were examined and the S/N determined by comparing the RMS signal power to the noise power observed by the detector when viewing a non-scintillating target at room temperature. In addition, where it could be measured, we compared the correlation of scintillation frequency and the mean of the absolute value of the crosswind. These results are summarized in Table I. Except for somewhat lower values for the higher paths to the telephone pole and the mountain horizon, C_n^2 ranged from 10^{-13} to 10^{-12} $m^{-2/3}$ during the tests.

Table I

Target	Date	Time	Range	SNR	normalized crosswind correlation 1.5 min periods
Hot plate (back side)	9/26	1630	80 m	21	0.66
Telephone pole against blue sky background	9/28	1139	120 m	1.2	--
		1200		1.2	
40 W soldering iron		1300	80 m	3.2	0.40
Looking at trailer window		1340	500 m	1.2	0.30
Telephone pole against sky					
Pole in sunlight, cloudy bright background		1600	120 m	3.4	--
Sun under cloud, cloudy bright background		1610	120 m	2.5	--
Mountain horizon		1621	12 km	2.4	--
Soldering iron at focus of 15-cm mirror		1639	500 m	12	0.40
		1644		6.7	0.35
	9/30	1039		28	0.50
		1109		37	0.55
		1125		27	0.40
		1500		13	0.40
Mountain horizon		1530	12 km	0.24	--
Telephone pole against blue sky background		1545	120 m	0.44	--
Edge of trailer		1605	500 m	0.24	0.10
Soldering iron at focus of 15-cm mirror		1630		41	0.80
		1635		31	0.50
		2045		9.3	0.80

4. DISCUSSION

The experimental results generally agree with the predictions. Clearly a 10 μm system can be built that will operate on selected targets. Because there is less contrast in the infrared scene and because infrared detector noise is somewhat higher, the effective SNR for this measurement is about two orders of magnitude below that of a system operating at 0.8 μm and observing an average scene on a sunny day. The best SNR was obtained experimentally on natural targets warmed by the sun and silhouetted against the clear blue sky high above the horizon. Additional information in natural background contrast is contained in the reference by Ashley et al. (1975). The infrared system will in principle, operate at night, although the SNR is reduced both because of lower C_n^2 and smaller temperature differences in the scene than are obtained in sunlight.

The improved instrumentation developed during this project is capable of wind measurement when the SNR is less than one. Of course the integrating time must be increased and the measurement becomes more sensitive to instrument movement and movement in the scene itself.

The wide range of C_n^2 and contrast that either wavelength passive system can encounter in operation makes it difficult to guarantee satisfactory operation of this kind of instrument. At the same time, it is by no means clear that the real limits of operation have been approached. More sophisticated multiple-aperture systems may well be capable of operating under much less favorable conditions than are required for the present designs.

5. REFERENCES

Ashley, G. W. et al. (1975): Background spectral radiance and contrast in the near-UV, mid-IR, and LWIR regions, General Dynamics/Pomona TM6-125PH-438 July 1975.

Clifford, S. F., G. R. Ochs and Ting-i Wang (1975): Optical wind sensing by observing the scintillations of a random scene, *Appl. Opt.*, 14:403-408.

Lawrence, R. S., G. R. Ochs and S. F. Clifford (1972): Use of scintillations to measure average wind across a light beam, *Appl. Opt.*, 11:239-243.

Ochs, G. R. and G. F. Miller (1972): Pattern velocity computers-two types developed for wind velocity measurement by optical means, *Rev. of Sci. Instr.*, 43:879-882.

Ochs, G. R., E. J. Goldenstein and R. F. Quintana, A second-generation passive optical crosswind monitor.

Wang, Ting-i, G. R. Ochs and S. F. Clifford, A saturation-resistant optical scintillometer to measure C_n^2 (Accepted for publication, JOSA; tentative issue: March 1978).